Contents

1 General context

1.1 Neutrino physics

1.1.1 A brief history of the neutrino

The existence of neutrinos was first postulated by W. Pauli in 1930 **[ref?]** to explain the continuous energy distribution of the β-decay while preserving energy conservation. It needed to be a neutral, light-weight fermion, hence the name neutrino (the little neutral in Italian). After its first observation (an electron antineutrino) by the Savannah experiment in 1956 **[ref?]**, multiple experiements in the second half the 20th century led to a good understanding of the particle while being theoritically described in accordance by the Standard Model (SM) of particle physics. In the SM, the neutrino is a massless, left-handed (antineutrino is right-handed), neutral lepton coming in three flavors: electronic ν_e, muonic ν_μ and tauic ν_τ. It interacts through weak interaction only and has a very small cross section of $\sim 10^{-38}\,\mathrm{cm}^2$, making it really tricky to detect.

However this picture has its imperfections, in 1970 the Homestake experiment detected only 40 % of the predicted electron neutrinos in the solar neutrino flux **[ref?]**. The Super Kamiokande Neutrino Detection Experiment in 1998 and the Sudbury Neutrino Observatory in 2002 [3] confirmed this discrepancy and established the existence of a new physical phenomenon theorized by B. Pontecorvo in 1967: neutrino flavor oscillations. The capacity for neutrino to oscillate between flavors during propagation is incompatible with the SM for at least two reasons: it violates total lepton number conservation and it requires non-zero neutrino masses.

The number of neutrino masses is not fully established, a forth (or more) neutrino mass eigenstate could exist in the form of a sterile neutrino(s). In the following, only three neutrino masses (m_1, m_2, m_3) are considered. They have never been directly accessed but an upper bond of 0.9 eV have been established **[ref?]**, only constraints on the mass differences $\Delta m^2_{ij} \equiv m^2_i - m^2_j$ could be set. As of today, two of theme have been measured leaving two possible mass hierarchy: normal order (NO) ($m_3 \gg m_2 > m_1$) and inverted order (IO) ($m_2 > m_1 \gg m_3$).

Two beyond SM formulations of a massive neutrino are in competition. The Dirac formulation consists of adding two degrees of freedom in the form of a right-handed sterile neutrino and preserves the lepton numbers conservation. The Majorana formulation postulate that neutrino and antineutrinos are undistinguishable and thus that lepton numbers are not conserved quantities. The Majorana nature of the neutrino is curretly the favored solution and is currently tested by searching for a neutrinoless double β-decay ($0\nu2\beta$) which would effectively violate the electronic lepton number [4].

1.1.2 Neutrino oscillations

Neutrino oscillations are described by a difference between the mass eigenstates ($i = 1, 2, 3$) at work during propagation, and the flavor eigenstates ($\alpha = e, \mu, \tau$) at work at the interactions. The unitary transformation relating the two eigenstate states is written as the unitary Pontecorvo-Maki-Nakagawa-Sakata (PMNS) mixing matrix U. The PMNS matrix can be parameterized by three mixing angles: θ_{12}, θ_{23}, θ_{13} as well as one Dirac phase: δ and two Majorana phases: α_1, α_2. Three additional non-physical phases can be absorbed in the lepton fields and the two Majorana phases do not affect oscillations and are thus ignored in the following [3]. We can then write the realtion between the two sets of eigenstates as:

$$|\nu_\alpha\rangle = \sum_i U^*_{\alpha i}|\nu_i\rangle \quad \text{with} \quad U = \begin{pmatrix} 1 & 0 & 0 \\ 0 & c_{23} & s_{23} \\ 0 & -s_{23} & c_{23} \end{pmatrix} \begin{pmatrix} c_{13} & 0 & s_{13}e^{-\mathrm{i}\delta} \\ 0 & 1 & 0 \\ -s_{13}e^{\mathrm{i}\delta} & 0 & c_{13} \end{pmatrix} \begin{pmatrix} c_{12} & s_{12} & 0 \\ -s_{12} & c_{12} & 0 \\ 0 & 0 & 1 \end{pmatrix}$$

where the PMNS matrix has been explicitly written as a product of three rotation matrix and using the convention: $c_{ij} \equiv \cos\theta_{ij}$ and $s_{ij} \equiv \sin\theta_{ij}$. One can now compute the propability for muon neutrinos of energy $E \simeq p$ to oscillate to an electron neutrino over a distance $L \simeq t$ in vacuum (working in natural units: $\hbar = c = 1$). Using a quantum mechanical framework, it suffices to express the neutrino states in term of the mass states which are Hamiltonian eigenstates by definition:

$$|\nu(t=0)\rangle \equiv |\nu_\mu\rangle = \sum_i U^*_{\mu i}|\nu_i\rangle \quad \text{and} \quad |\nu(t)\rangle = \sum_i U^*_{\mu i} e^{-\mathrm{i}E_i t}|\nu_i\rangle$$

Where the energy E_i can be written as: $E_i \equiv \sqrt{p^2 + m_i^2} \simeq p + \frac{m_i^2}{2p} = E + \frac{m_i^2}{2p}$. The propability of oscillations over L is as follows:

$$P(\nu_\mu \to \nu_e, L) = |\langle \nu_e | \nu(t) \rangle|^2 = \left| \sum_i U_{ei} U_{\mu i}^* \exp\left(-\mathrm{i} \frac{m_i^2 L}{2E} \right) \right|^2$$

After some computation, the final result at second order in small quantities $\sin\theta_{13}$ and $\sin(\Delta m_{21}^2 L/4E)$ is :

$$P(\nu_\mu \to \nu_e, L) = \alpha \sin^2\left(\frac{\Delta m_{31}^2 L}{4E}\right) + \beta \sin^2\left(\frac{\Delta m_{21}^2 L}{4E}\right) + \gamma \sin\left(\frac{\Delta m_{21}^2 L}{4E}\right) \sin\left(\frac{\Delta m_{31}^2 L}{4E}\right) \left(\frac{1}{2}\cos\delta - \sin\delta\right)$$

where α, β, γ are functions of θ_{12}, θ_{23}, θ_{13} only [3]. From this formula, two pieces of information will be of importance in this manuscript. Firstly, oscillation probability peaks and vanishes as a function of L/E, and secondly, oscillation experiements only give information on the mass differences Δm_{ij}^2 and cannot access absolute mass values.

On another hand, this paradigm allows to quantify charge conjugation and parity (CP) violation in neutrino oscillations by looking at the difference $P(\nu_\alpha \to \nu_\beta) - P(\bar{\nu}_\alpha \to \bar{\nu}_\beta)$. It can be shown that this difference is proportional to the sinus of the Dirac phase δ (when $\alpha \neq \beta$) [3]. It is thus commonly referred as the CP violation phase δ_{CP} as a zero value would imply CP conservation. To be more precise, all mixing angles and mass differences must also be non-zero but this a necessary condition for the already observed three flavor oscillations while δ_{CP} is yet fully unknown.

When neutrinos travel through matter we have to take into account an additional potential coming from the charged current interaction of ν_e with matter electrons. Those interactions are absent from the muonic and tauic sectors as muons and tauons don't appear in regular matter. Moreover, neutral current interactions are equivalent for all three flavors and do not impact the oscillation mechanism. Propagation in constant-density matter will have an effect of resonant effect of oscillations depending on density and will either enhance neutrino or antineutrino oscillations between two flavors at resonance depending on the sign of Δm^2. This property can thus give us access to the sign of Δm_{31}^2 and to the mass hierarchy [3].

are we at density resonance in DUNE ?

1.2 The Deep Underground Neutrino Experiment

The Deep Underground Neutrino Experiment (DUNE) is an international collaboration involving more than 1400 collaborators from over 200 institutions in over 30 countries without several research goals [2].

1.2.1 The DUNE physics program

High-precision measurement of the various parameters involved in neutrino flavor oscillations could determine the sign of Δm_{31}^2 effectively fixing the mass ordering as well as the octant of θ_{23} **why it matters ?** in addition to lower incertitudes on already measured quantities.

Investigating CP violation in the lepton sector with high-precision measurement of δ_{CP} by comparing neutrino and antineutrino oscillations. This could shed light on baryogenesis as CP violation is one of the three Sakharov conditions that must be satisfied by a process generating matter and antimatter at different rates.

The detection of galactic core collapse supernova neutrino bursts requires good sensibility in MeV-energy and a good understanding of the energy and time signature of such a signal. Neutrino being the first messengers to reach earth in a supernova, DUNE will be part of the SuperNova Early Warning System (SNEWS) and set off an early alert of a galactic supernova event for observatories minutes to hours before the supernova electromagnetic signal reaches Earth. This network would allow to measure the first seconds of the supernova electromagnetic signal which contains information about what occurred in the core of the star [5].

Searching for an hypothetical proton decay $p \to K^+ \bar{\nu}$ requires identifying the short kaon tracks in the background induced by cosmic muons, and a good time resolution [1].

1.2.2 Installation

The DUNE final installation is located in the United States of America, is composed of a muon neutrino beam and a near detector at the Fermi National Accelerator Laboratory (Fermilab) near Batavia, Illinois, and a far detector at the Sanford Underground Research Facility (SURF) in Lead, South Dakota (cf. Figure 1).

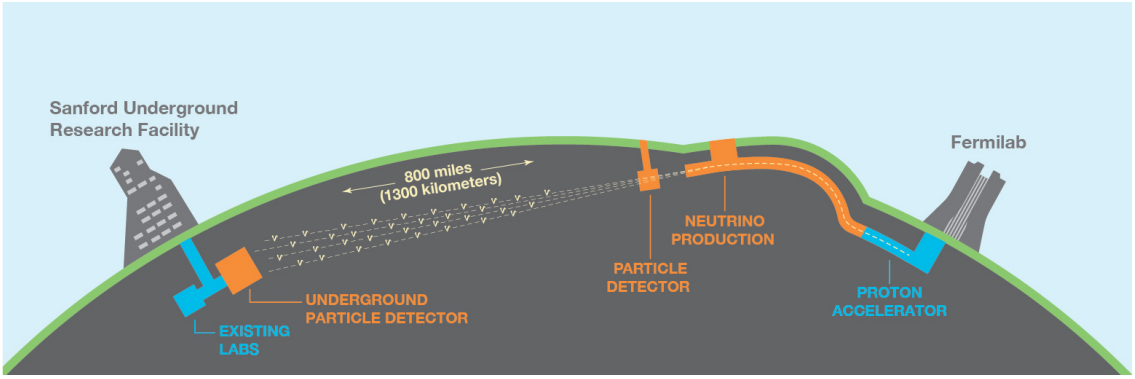

Figure 1: DUNE installation. From left to right: the far detector at SURF, the near detector and the proton accelerator at Fermilab [2].

The Fermilab 1.2 MW main injector produces a 120 GeV proton beam hitting a large target producing a shower of hadrons (mostly pions) then focused by three 300 kA magnetic horns into a 200 m long decay pipe. 99.9 % of the charged pions will decay into muons and muon neutrinos which will then travel to the near detector 400 m downstream. The horns current polarity can be swapped to select only positive or negative pions (with 10 % contamination) leading in a muon neutrino or muon antineutrino beam respsectively. This will allow seperate measurement of neutrino and antineutrino oscillation which crucial to the determination of δ_{CP}. An additional 1 % contamination of electron neutrinos from kaons and muon decays is expected. The near detector aims to measure the beam parameters and is near enough to the beam to presume no neutrino flavor oscillation in the beam allowing to isolate the effect of the oscillation. The far detector is located 1285 km downstream of the beam and 1480 m underground in a former gold mine. It is composed of four liquid argon time-projection chambers (LArTPC) for a total of 40 kt of fiducial volume. The four LArTPCs will use two similar technologies, namely two vertical drift (VD) and two horizontal drift (HD).

1.3 The DUNE group at IJCLab

This intership was carried out at the Irène Joliot-Curie laboratory (IJCLab) in Orsay, France, from the National Institut of Nuclear Physics and Particle Physics (IN2P3) from the French National Center for Scientific Research (CNRS). The group working on the DUNE project is composed of three permanant researchers: Thibaut Houdy, Yoanne Kermaïdic and Fabien Cavalier and two Ph.D. students: Emile ... and Matteo ...

Data analysis at IJCLab

The group is in charge of the design and production of the chemineys hosting the electronic devices responsible for the outgoing data at the top of the vertical drift detectors, as well as the printed circuit board (PCB) interface between the LAr and the outside. The chemineys located at the bottoms are handled by **who?**. Under the direction of Dr. Houdy, this intership aims at developping the analysis of Michel electrons in the prototype detector alongside other collaborators: Matteo Galli at the Astroparticle and Cosmology (APC) laboratory in Paris, France, and Laura Pérez Molina at the Centre for Energy, Environmental and Technological Research (CIEMAT) in Madrid, Spain.

2 The ProtoDUNE experiements at CERN

2.1 Presentation

Various LArTPC prototypes (ProtoDUNE) are being built and operated the neutrino platform at the European Organization for Nuclear Research (CERN). SP/VD/HD

VD data at the end of 2024

2.2 Vertical drift technology

The group at IJCLab is specialized in the vertical drift technology, the ProtoDUNE-VD at CERN is m width, m depth and m height.

composed of two anodes in the top and bottom of the TPC and a cathode suspended halfway up creating two 6.5 m vertical drift volumes. The cathode is set at **???**0 kV while the anodes, in direct contact with the entire cryostat, are set to the ground. The electrons ionized by the charged particles will drift up in the upper volume and down in the lower volume under the influence of the 0 kV/cm electric field. The active volume is surrounded by a field cage **why ?**. By convention the drifting axis is the x-axis and the beam axis is the z-axis.

The cathode is divided in chuncks intependantly suspended. Each chunk is composed as grid of [**material ?**] with evenly distributed **Arapuca PD** in some of the square holes. The LAr can freely move from top to bottom of the TPC maximazing the total active volume.

The anodes are each composed of three charge-readout planes (CRP) immersed in the LAr. Multiple holes allow the drifting electrons to pass through each layer while evenly spaced stripes and their surfaces are used to tag their passage. The first two layers, U and V, are induction planes set at **???**0 kV and **???**0 kV respsectivley. They stripes form an angle of $-35°$ and $+35°$ with the stripes of the collection plane respsectivley. Charged particles passing through the induction planes are tagged by the bipolar (zero integral) signal in the nearest stripe. The outermost layer, W, is a collection plane set at **???**+0 kV which will collect the drifting electrons resulting in a unipolar (positive integral) signal. The conjugation of the induction plane signals allow the reconstruction of the position of the energy deposit in the yz-plane while the collection plane has the best signal-to-noise performance and charge resolution and is thuse used to reconstruct the electron energy [7].

A photon detection system (PDS) is used to tag an initial time point at the reception of the scintillation photon. The collected electron being thermalized, their drift speed is determined by the applied electric field. The elapsed time between photon and electron reception allow to reconstruct the x-position of the energy deposit by the charged particle.

Arapucas

The maximal energy sensibility of the far detector is set to 2.6 GeV to maximize the $\nu_\mu \to \nu_e$ oscillation probability by adjusting the ratio E/L

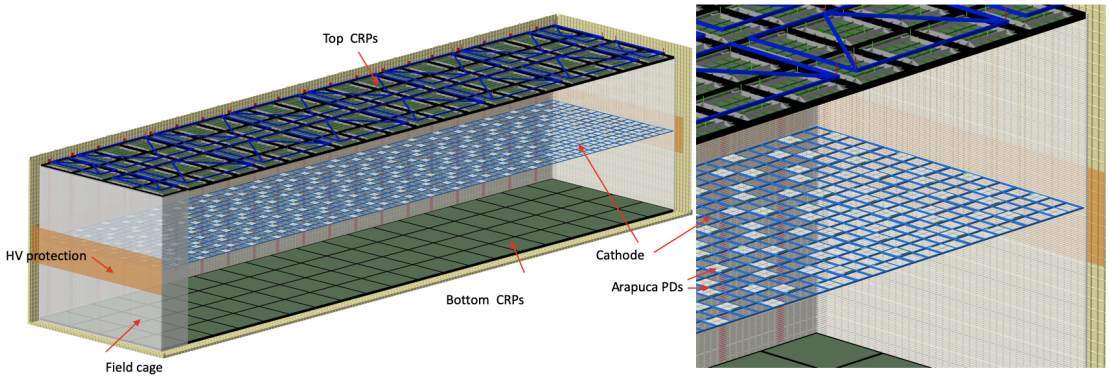

Figure 2: [1]

2.3 Liquid argon

The chosen detector technology for the far detector is large modules of liquid argon (LAr), acting as a scintillators, contained in a cryostat at $-184\,°\mathrm{C}$. LAr

A charged particle through-going LAr deposit energy *via* ionizing the Ar atoms and *via* excitation [7]. The ionization energy of the Ar being 20 eV, a typical cosmic muon with a $\mathrm{d}E/\mathrm{d}x$ of 2 MeV/cm would ionize up to 200,000 electrons per centimeter which would in turn inonize more Ar atoms creating so-called electromagnetic showers in the scintillator. The ionized argon atoms Ar^+ will form molecular bond Ar_2^+ with neutral Ar atoms before recombining with surrounding free electrons to excimers Ar_2^*. In absence of exterior electric field, the charged particle will most likely only excite Ar atoms creating Ar_2^* without free ionized electrons. Higher the electric field, More easily the Ar atoms will be ionized. The excimers will return to the fundamental state 2Ar by dissociating and emitting scintillation UV photons of 128 nm of wavelength. Figure 3

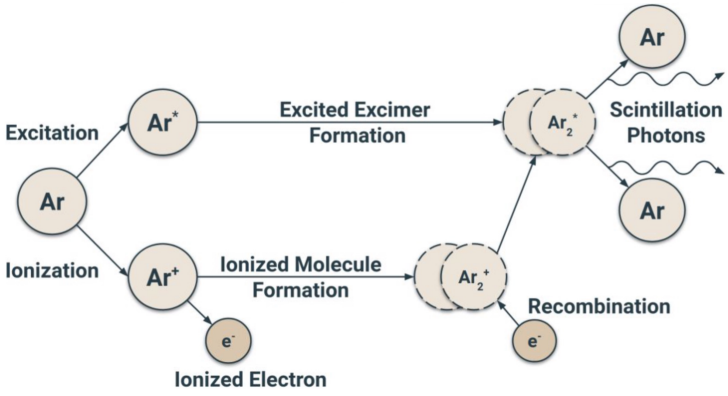

Figure 3: **[ref?]**

Those photons can propagate freely in the LAr as it is transparant at this frequency in absence of impurity. This also mean that the mean free path of scintillation photons can be a measure of the liquid purity. Dopping LAr with Xe is studied as it would act as a wavelength shifter by absorbing the

electrons: radiative losses, namely bremsstrahlung radations (continuous specter). The emitted photons have a typical energy of tens of keV and will be reabsorbed by the medium and inonize electrons through the photoelectric effect.

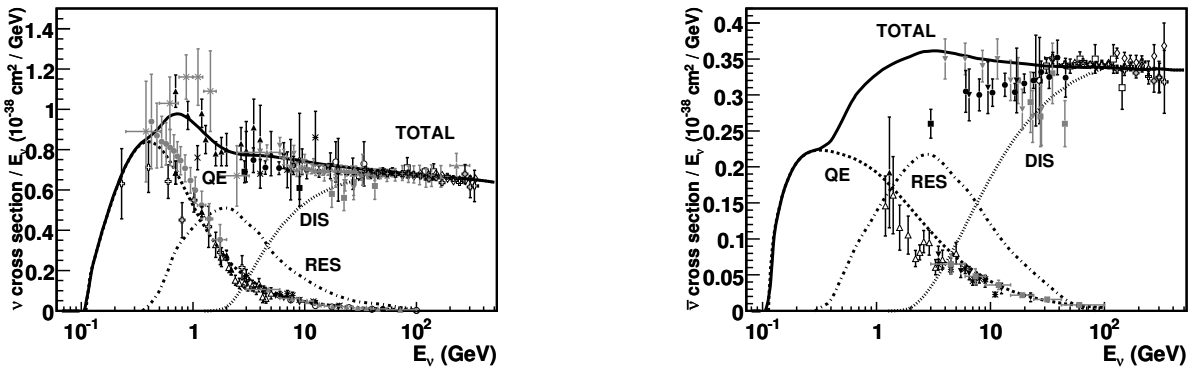

Figure 4: Total neutrino and antineutrino per nucleon charged current cross sections (for an isoscalar target) divided by neutrino energy and plotted as a function of energy. [6]

neutrino interaction channels

3 Michel electron tracks reconstruction

3.1 Michel electrons

In the main muon decay channel $\mu^{\pm} \to e^{\pm}\nu_{\mu}\nu_{e}$ (ν and $\bar{\nu}$ undistinguished), the electron (or positron) is called a Michel electron. Michel electrons are theoritically well-known and their energy is continuously distributed between 1 to 50 MeV, making them a good candidate for low energy calibration of the LArTPCs.

Extensive study of the Michel electrons have been carried out in the ProtoDUNE-SP detector [7] **Aleena**. A list of criteria has been used to select Muon tracks and identify Michel electron candidates. One of them proposed to determine the endpoint of a muon track, an the starting point of the Michel electron track, by searching for a sharp angle under 130° in the reconstructed track. While this method proved its effectiveness it exclude many potential Michel electron candidate which go in the same direction of the initial muon. This intership will invistigate an other method: looking at the energy deposit as a function of the track length of the muon. A cosmic muon has mostly a constant energy deposit $\mathrm{d}E/\mathrm{d}x$ of 2.1 MeV/cm in LAr but it diverges immediatly before the muon comes to rest and decay forming what is known as a Bragg peak (cf. Figure 5). The idea is to use this phenomenon to tag the endpoint of muon tracks and consider the continuation of the track beyond the Bragg peak as a candidate Michel electron track.

Quenching: for the same $\mathrm{d}E/\mathrm{d}x$, two different particle deposit their energy through different channels.

Taking into account the shielding of drifting electrons, and more importantly the heavy, slow ions on the local exterior electric field (on Ar inonization/scintillation ratio, and electron drifting trajectories/speed)

Figure 5: Energy deposit per distance of a muon with respect to the track lenght. Shortly before the endpoint of track, the energy deposit per distance diverges forming a Bragg peak.

3.2 LArSoft

The liquid argon software (LArSoft) is a set of programs using the ROOT library used for all the steps of data analysis important to DUNE: from fake data generation to track reconstruction.

The first step is generating incoming particles and their initial parameters: energy, momentum (direction)and position. The Cosmic Ray Simulationfor Kaskade (CORSIKA) program provides extensive simulation for air showers initiated by high energy cosmic ray particles.

The next step consists in simulating particle propagation through LAr, computing their energy deposits and trajectories. Then, the following ionizations, scintillations, as well as electromagnetic showers and light matter interaction are performed. Those two steps are both handled by the Geometry And Tracking (Geant4) program using Monte Carlo methods.

Once the interactions with the medium is computed, the Wire-Cell Toolkit (WTC) simulate the detector response. At this stage the simulated data should be similar to what is expected to come out of the data acquisition systems (DAQ) (after a necessary stage of data conversion) in real-world experiemntal situation.

This final step is common to simulated and experiemental data. The reconstruction stage build three-dimensional particle tracks from the detector output. **(particle identification ?..., computaion of energy deposit etc.)** Such software as Pandora and GaussHit,

References

[1] DUNE Collaboration, ?. ?, *Title*, ?.

[2] dunescience.org

[3] C. Giganti, S. Lavignac and M. Zito, *Neutrino oscillations: the rise of the PMNS paradigm*, 2017. arXiv:1710.00715

[4] S. M. Bilenky, *Neutrinos: Majorana or Dirac?*, 2020. arXiv:2008.02110

[5] arXiv:2011.00035

[6] J. A. Formaggio and G. P. Zeller, *From eV to EeV: Neutrino Cross-Sections Across Energy Scales*, 2013. arXiv:1305.7513

[7] *Identification and reconstruction of low-energy electrons in the ProtoDUNE-SP detector*, arXiv:2211.01166